



Treball Final de Grau

Control of colloidal systems by means of thermoresponsive polymers

Control de sistemes col·loïdals mitjançant polímers termosensibles

Raimon Terricabres Polo

June 2019



UNIVERSITAT DE
BARCELONA

B · KC Barcelona
Knowledge
Campus
Campus d'Excel·lència Internacional

Aquesta obra està subjecta a la llicència de:
Reconeixement–NoComercial–SenseObraDerivada



<http://creativecommons.org/licenses/by-nc-nd/3.0/es/>

*Since we cannot know all that there is to be known
about anything, we ought to know a little about
everything*

Blaise Pascal

Encara que en aquest treball només hi consti un autor, m'omple d'alegria poder dir que moltes persones hi heu posat el vostre gra de sorra i, per això, en part també és vostre.

Voldria agrair a en Francesc Sagués i en Jordi Ignés-Mullol la proposta d'un tema tant interessant com el dels cristalls líquids i el fet d'haver-me obert les portes del LAB 4017 de bat a bat.

Perquè la feina al laboratori no es fa sola, ni sol, us agraeixo a tu Ignasi, Berta i Josep Maria tots els consells que m'heu donat i el que hem compartit. Haguéssim pogut sortir més d'hora amb la feina feta però segur que no hauríem arribat tan lluny. També a vosaltres, Clara, Cristina, Anna i Dani pels bons moments i l'agradable companyia.

Un treball final de grau no només es cou al laboratori entre estudiants sinó també a casa i en família. Moltes gràcies Júlia, Sergi i David per fer-me més fàcil viure a Barcelona. Moltes gràcies als de casa, per animar-me a donar el màxim de mi i a gaudir de la feina ben feta.

Ja per acabar, voldria agrair a la Terra, i a la Plana en concret, tots els moments de desconnexió que m'ha regalat. Cuidem-la, només en tenim una i no ens agradaria sense allò que és i representa: vida.

REPORT

CONTENTS

1. SUMMARY	3
2. RESUM	5
3. INTRODUCTION	7
3.1. Liquid Crystals (LCs)	7
3.1.1. Classification	8
3.1.1.1. Thermotropics LCs	8
3.1.1.2. Lyotropic LCs (LLCs)	8
3.1.2. Lyotropic chromonic LCs (LCLCs)	9
3.1.2.1. LCLCs mesophases	9
3.1.3. LCs anchoring	10
3.1.4. Director field distortion in nematic LCs	11
3.1.4.1. Nematic droplets	12
3.1.5. LCs properties: anisotropy	12
3.1.5.1. Birefringence	13
3.1.6. LCs optical characterization	13
3.2. Poly(N-isopropylacrylamide) (PNIPAM)	13
3.2.1. Thermoresponsive character	14
3.2.2. PNIPAM based materials	15
3.3. Depletion force	15
3.3.1. Polyethylene glycol (PEG) as a depleting agent	16
4. OBJECTIVES	17
5. EXPERIMENTAL SECTION	19
5.1. Preparation of PNIPAM based materials	19
5.1.1. Synthesis of microgel particles	19
5.1.2. Glass functionalization	19
5.2. LCLCs solutions	20

5.3. Preparation of LC cells	21
5.3.1. Glass cleaning	21
5.3.2. PVA coating	21
5.3.3. Cell assembly	22
5.4. LC phases and LC transition study	22
5.5. Indirect size measurements	23
5.6. Contact angle measurements	24
6. RESULTS AND DISCUSSION	24
6.1. Thermoresponsive materials	24
6.1.1. Microgel particles	24
6.1.2. Functionalized glass	25
6.2. DLS measurements	26
6.2.1. PEG	26
6.2.2. PNIPAM	27
6.2.3. Size dependent depletion	28
6.3. LCLCs phases and transitions	29
6.3.1. DSCG-Water	30
6.3.2. PEG-DSCG-Water	30
6.3.3. PNIPAM-DSCG-Water	32
7. CONCLUSIONS	35
8. REFERENCES AND NOTES	37
9. ACRONYMS	39
APPENDICES	41
Appendix 1: Reagents and suppliers list	43
Appendix 2: Dynamic Light Scattering (DLS)	45

1. SUMMARY

Disodium cromoglycate (DSCG) molecules in water pack in stacks, whose length and liquid crystal (LC) phases depends on temperature, concentration and the presence of depleting agents. In the present work, DSCG-Water LC phases and phase transitions are studied in free-depletant, non-thermoresponsive depletant (polyethylene glycol, PEG) and thermoresponsive depletant (poly(N-isopropylacrylamide), PNIPAM) mixtures. Nematic (N) to isotropic (I) phase transition temperature is increased in the presence of these depleting agents. PNIPAM loses that property above the lower critical solution temperature (LCST), whereas PEG effect is not modified. Both polymers depleting capacity is also compared by dynamic light scattering (DLS) analysis, showing that PNIPAM applies a stronger depletion force than PEG of the same molecular weight at 25 °C. Finally, PNIPAM-functionalized surfaces and microgel particles have been synthesized and their thermoresponsive properties have been studied.

Keywords: Chromonics, liquid crystals, PNIPAM, depletion, thermoresponsive

2. RESUM

Les molècules de DSCG en aigua s'empaqueten en piles, la longitud i fases de cristall líquid de les quals depèn de la temperatura, la concentració i la presència d'agents depletius. En aquest treball, les fases de cristall líquid i les seves transicions s'estudien en mescles sense depletiu, amb depletiu no termosensible (PEG) i amb depletiu termosensible (PNIPAM). La temperatura de transició de fase nemàtica a isotròpica s'incrementa amb la presència d'agents depletius. El PNIPAM perd aquesta propietat per sobre de la LCST, mentre que el PEG no es veu modificat. La capacitat de depleció d'ambdós polímers també es compara per anàlisi de DLS, evidenciant que un PNIPAM exerceix un força de depleció més forta que un PEG del mateix pes molecular a 25 °C. Finalment, s'han sintetitzat superfícies funcionalitzades amb PNIPAM i partícules de microgel i se n'han estudiat les propietats termosensibles.

Paraules clau: Cromònics, cristalls líquids, PNIPAM, depleció, termosensible

3. INTRODUCTION

Control of colloidal systems is crucial for many industrial, technological and biological applications.¹ From mayonnaise to cosmetics through paints and drugs, they are present in every moment of our daily life. Colloids are described as a mixture of discrete particles in a dispersant substance. However, most of them consist on more than two substances, which makes the mixture more complex to control.

In many systems, colloids are mixed with polymers that can considerably affect their stability. In water-based systems, its stability also depends on the pH, temperature and ionic strength. Colloidal system properties rely on its stability, so it is essential to understand its destabilizing mechanisms. Flocculation induced by non-adsorbing polymers is the studied topic herein, which is common in latex-based paints and protein-polysaccharide products in food industry.^{2,3}

Besides direct industrial applications, there are numerous colloidal systems of great interests in cutting edge research, above all those related with new materials and molecular assemblies.⁴ In the cited and referent work, O. Lavrentovitch et al. studies a liquid crystal (LC) molecules assembly in a crowded medium, which could provide information about intracellular molecular assemblies.

3.1. LIQUID CRYSTALS (LCs)⁵

LCs are a phase of matter between a crystalline solid and an isotropic liquid. That is why they are used to be named mesophases, where *meso* means “between” in Ancient Greek.

They were first discovered 1888 by the Austrian botanical physiologist Friederich Reinitzer while studying cholesterol derivates phases transition. He found that cholesteryl benzoate does not melt like common solids, he found that two different melting points at 145.5 °C and 178.5 °C respectively. Heating the solid, a cloudy fluid was obtained from the first transition whereas the second one lead to a clear liquid. This was the beginning of a new promising field, whose study was conducted by their discoverer, von Zepharovich and Otto Lehmann, who coined the name “liquid crystal”. They studied the crystalline character of the mesophase and important optical properties involving the ability to rotate the polarization of light.

It was not until the 1960s that LCs had its first application, as since then they were just of scientific curiosity. Their unique properties allowed the design of liquid crystal displays, nowadays found in smartphones and computers.

LCs are characterized for not having a translational order but a mean orientational one. As explained before, its structure is a combination of a crystalline solid, orientationally and translationally ordered, and an isotropic liquid, non-ordered phase. The main orientational axis is called director field and is described as \vec{n} .

3.1.1. Classification

Hundreds of LCs have been synthesized since their discovery. Some of them are pure substances, others are mixtures. Overall, they are classified depending on how they reach the mesophases and what rules their transitions. Sometimes, an extra class of LCs called metallotropic is added, although there is no studied in deep.⁶

3.1.1.1. Thermotropic LCs

Thermotropic LCs are pure substances or mixtures of them whose mesophases are obtained while heating their solid or cooling their liquid phase. Cholesteryl benzoate is an example of thermotropic LCs. They can organize in diverse mesophases depending on their molecular structure and intermolecular interactions: cholesteric, nematic, smectic and columnar.

3.1.1.2. Lyotropic LCs (LLCs)

LLCs form orientationally organized mesophases depending on temperature and solvent-solute interactions, so they are mixtures of substances. Increasing solute concentration will enhance the formation of condensed phases, whereas diluting it will diminish particle assembly.

Amphiphilic linear molecules organize in micelles above a certain concentration called *cmc* (critical micelle concentration). The solute consists on a long apolar chain ended in a polar head. Soaps and phospholipids are broadly known examples of water-based LLCs. Increasing solute concentration can induce to other condensed structures like bilayers and hexagonal assemblies.

Lyotropic chromonic LCs (LCLCs), another type of LLCs, are characterized for their self-assembly behaviour in crowded solutions. They are especially studied for potential biological applications, they are non-toxic and biologically friendly systems. LCLCs can be obtained by dissolving dyes (Sunset Yellow) or pharmaceutical active ingredients (Cromolyn) in water.

3.1.2. Lyotropic chromonic LCs (LCLCs)

LCLCs are differentiated from other LLCs for their assembly units. They are disk-like or plant-like molecules instead of linear ones. They have an aromatic flat inner core and polar groups at the periphery. As seen in the studied compound (Figure 1), disodium cromoglycate (DSCG) has two carboxylate groups at their ends and aromatic rings in the inner parts. In water solution, molecules are packed in stacks, assembling aromatic rings on top of each other and polar groups at the outer face, stabilized by ion-dipolar interactions with water.

When solved in water, the length of the DSCG stacks is increased at high concentrations and at low temperatures. The gap between molecules is 3.4 Å and the section of the stack 11.5x16.0 Å.⁷

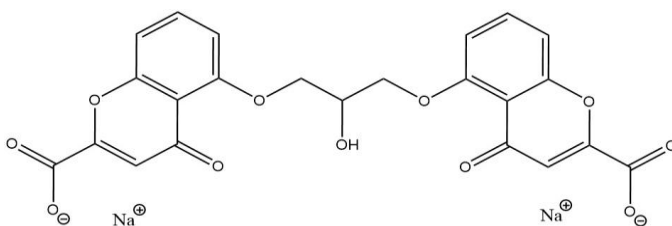


Figure 1. DSCG molecular structure.

3.1.2.1. LCLCs mesophases

DSCG-Water phase diagram (Figure 2) consists of three monophasic and three biphasic regions. Each one has a specific structure depending on stacks' length and density.

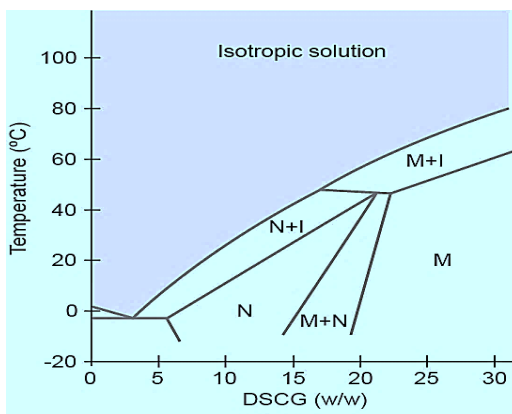


Figure 2. DSCG-Water phase diagram.

In all the following described phases water and DSCG, which none of them are pure substances.

- Isotropic(I): A homogeneous fluidic phase, where stacks length is variable. There is no orientational nor translational order. The fluid behaves like an isotropic liquid, although it is more viscous than water.
- Nematic (N): DSCG stacks are long and concentrated enough to generate condensed phases. The packing units have a mean orientational order, described by the field director. There is none translational order, as shown in Figure 3.
- Hexagonal (M): It is also called hexagonal columnar packaging in some literature.⁸ Stacks are longer in M than in N phase and are packed in hexagonal lattices. The main columns orientation is more defined than in N phase.

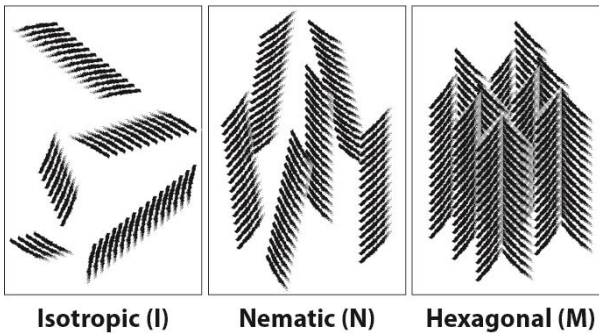


Figure 3. LCLC phases and stacks packaging.

The DSCG-Water system also shows phase coexistence in thermodynamic equilibrium, where phase domains depend on the composition, initial conditions and transformations. In those conditions, several geometric structures arises like tactoids, toroids and spherical drops.⁴

3.1.3. LCs anchoring⁹

LCs anchoring refers to the interaction and directors field deformation at an interface. Depending on the contacting material, the \vec{n} angle with respect the surface, anchoring, is classified in three categories (Figure 4):

- Homeotropic: LCs units are oriented perpendicular to the surface.
- Planar: Stacks are oriented parallel to the surface. It can be homogeneous if all the stacks are oriented in the same direction or degenerate if not.

- Tilted: Director field is oriented at a polar angle between 0° and 90° , a middle range character between planar and homeotropic.

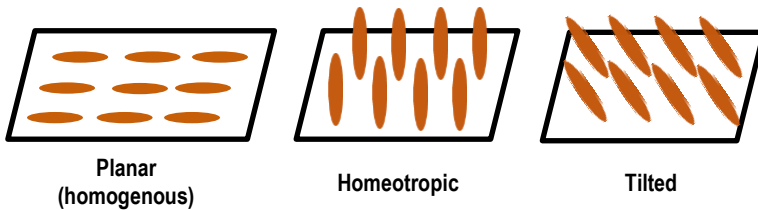


Figure 4. LCs anchoring representations.

3.1.4. Director field distortion in nematic LCs

Nematic phases are characterized for having a mean orientational order (\bar{n}). In absence of external or internal constraints, the orientational axis is uniform throughout the mesophase, since it corresponds to the minimum energy state. However, it can be distorted by external fields, boundary conditions and solid particle mixed in the matrix.⁵

The elastic continuum theory, a mathematic model, treats it as a continuum material, ignoring the molecular details. Thus, deformations are described as elastic distortions of the director field. In a uniaxial oriented system, there are three types of elastic deformation (Figure 5). Bend and splay are two-dimensional deformations whereas twist is a three-dimensional one.

Each deformation has associated an elastic constant value, which is characteristic of a given LC. Depending on their values, the nematic phase would tend to distort in a certain way, the minimum energy one.

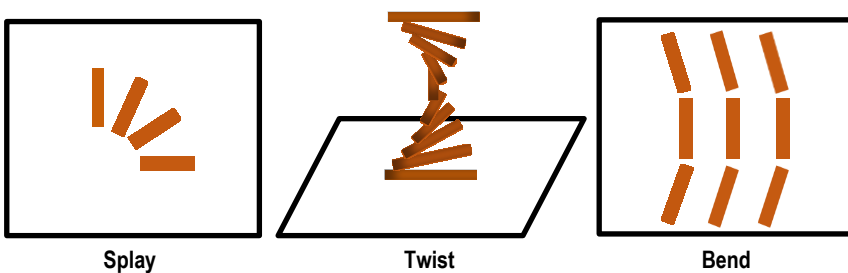


Figure 5. LCs director field elastic distortions.

3.1.4.1. Nematic droplets

As explained before, phase coexistence leads to special geometric domains. In the case of N-I coexistence, condensed areas shape and organization relies on the anchoring and elastic properties of the material.¹⁰

Nematic droplets are classified in four spherical configurations (Figure 6), whose director field orientation determines how they will be identified under a polarized optical microscope (POM).

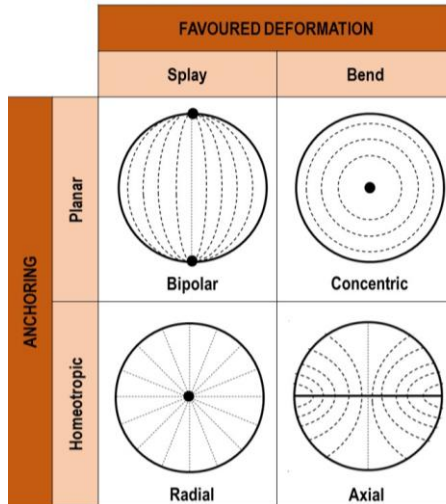


Figure 6. Nematic droplets configuration depending on predominant elastic distortion and surface anchoring. Director field marked with dashed lines.

Besides spherical drops, other shapes like tactoids are found in N-I. They are classified as positive tactoids, a nematic drop in a continuous I phase, and negative tactoids, an isotropic drop in a N continuous phase.¹⁰ Tactoids shape arises from a competence between surface tension, anchoring strength and the bulk elastic energy. The size of the tactoid will determine which of the three forces rules. The smaller the tactoid, the more deformed it will be due to surface tension. The bigger the tactoid, the more spherical-like will be as surface tension will decrease in detriment to the bulk elastic forces.¹¹

3.1.5. LCs properties: anisotropy

The uniaxial symmetry around the director field leads LCs to anisotropy in many properties. It means that dielectric permittivity values, for example, depends on their orientation with respect

to the \vec{n} . Thus, parallel and perpendicular measured values are remarkably different. Anisotropy affects refractive index, magnetic susceptibility, viscosity and conductivity basically.

3.1.5.1. Birefringence

Birefringence is a consequence of the optical properties' anisotropy. Different refractive index values cause light polarized along the director to propagate at different velocity than light polarized perpendicular to it (Figure 7). When light exits the material, two components are generated that have travelled at different velocities the same distance. It induces a phase retardation (Γ), which depending on their value will produce linear ($\Gamma=k\pi$, being k a natural number), circular ($\Gamma=k\pi/2$) or elliptical ($\Gamma \neq k\pi/2$) polarized light.

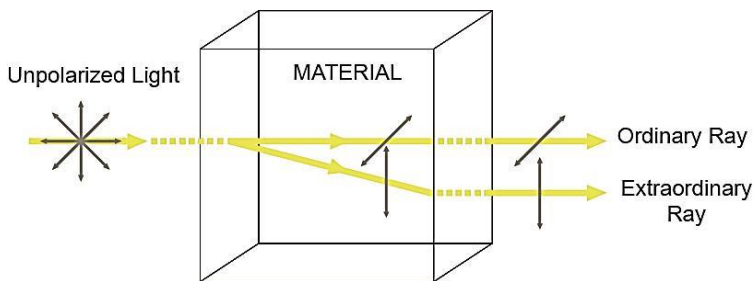


Figure 7. Light interaction with a birefringent material.

3.1.6. LCs optical characterization

Observing LCs ordered phases between crossed polarizers reveals the director field at a macroscopic level. I phase is seen completely dark in a polarized optical microscope (POM) as it does not interact with light. On the other hand, birefringent phases will appear bright as they interact with the light before it passes through the second polarizer. These phases are also detected by rotating the slide, as birefringent phases image will rotate because of the relative position of the director field with respect the polarized light.

3.2. POLY(N-ISOPROPILACRYLAMIDE) (PNIPAM)

First time synthesized in the 1950s, PNIPAM was patented as a rodent repellent.¹² In 1968, Heskins, M. et al. discovered the unusual thermoresponsive behaviour of PNIPAM-Water solutions.¹³

PNIPAM is synthesized from the monomer N-Isopropylacrylamide (NIPAM) via free-radical polymerization in water.¹⁴ Other paths using ultrasounds, radiation, Lewis acids and distillation-precipitation methods have succeeded.^{15,16,17,18} It is non-toxic although the monomer is harmful, that is why synthetic procedures are always followed by an accurate purification.

3.2.1. Thermoresponsive character

In solution, the polymer forms a three dimensional hydrogel which undergoes a phase separation above 32 °C.¹³ This property rapidly attracted the scientific community attention as it will behave as a smart material at inner body temperatures.

When dissolved in water at room temperature, PNIPAM swells and spread forming a viscous hydrogel. However, when heated above 32°C it undergoes a reversible lower critical solution temperature (LCST) phase transition. The resulting biphasic system consists on shrink polymer chains suspended in water. As shown in Figure 8a, polymer chains go through considerably a size change.

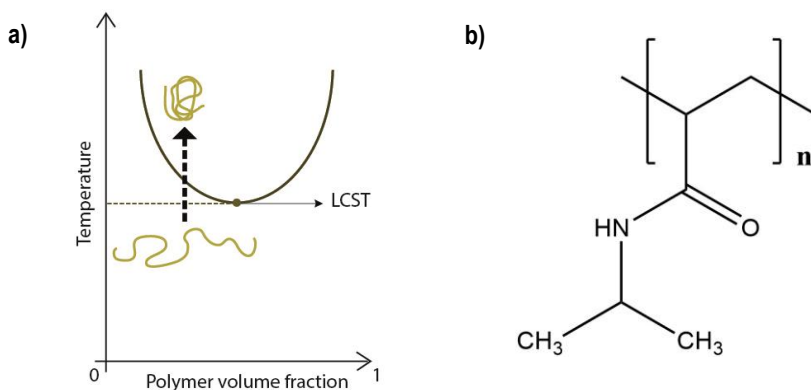


Figure 8. a) PNIPAM LCST phase transition from a swollen to a shrink chain. b) PNIPAM molecular structure.

This transition can be described at molecular level by the interactions between PNIPAM and water. Below LCST, amide groups form hydrogen bonds with water, therefore the chain is well extended. Above that temperature, amide groups establish hydrogen bonds with each other and fold small.¹⁹ The reason why does it happen at 32 °C is not clear, although some theoretical models obtained trust values considering chain rearrangement and coil-to-globule transition interactions.²⁰

LCST can be tuned by modifying the polymer or the medium. When combined with a non-thermoresponsive polymer, the resulting copolymer have softer properties and LCST decreases. It also depends on the molecular weight (chain length), functional groups (polar or non-polar) and polymer volume fraction in solution. Regarding to the medium, crowded and confined systems are related with low LCST values. Ionic strength, especially due to anions, decrease its value also.¹⁹ Overall, there is not an exact reference value for the phase transition, but it is used located between 28 and 32°C.

3.2.2. PNIPAM based materials

The thermoresponsive character of this material has inspired potential applications in biomedicine. When spread, polymer chains act as delivery box containing cells, drugs or nutrients.²¹ When shrink, they expel the content on the targeted tissue or organ. It has also been studied as a potential artificial tissue, according to its biocompatibility.²²

On PNIPAM grafted surfaces, LCST phase transition is associated with hydrophilic-hydrophobic behaviour. The coating is hydrophilic when the polymer is spread and hydrophobic when it shrinks.²³ That property is desired for water-proof and auto-cleaning surfaces.

3.3. DEPLETION FORCE²⁴

When adding a non-adsorbing polymer to a colloidal system, it induces phase separation. In the crowded solution, colloidal particles experiment an attractive force with each other provoking flocculation.

It is an entropic force, so the phenomenon arises from the entire system's statistical tendency to increase entropy. Contrary to what would be expected, colloids aggregation is entropically favourable in these systems.

As Figure 9 shows, there is an excluded volume for the polymer around the large particles, at a certain distance from their surface, the polymer radius of gyration (R_g). The polymer is lyophilic, so it is entropically favourable to spread along the whole solution, with no-excluded zones. Thus, when two excluded volume regions overlap, excluded volume decreases and polymer's entropy increases. It induces an attraction force between the particles that reduces the excluded volume, resulting in system's entropy increment.

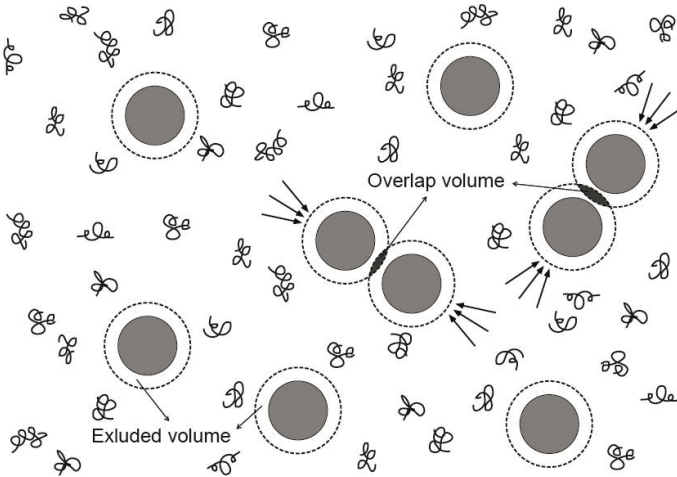


Figure 9. Crowded colloidal system formed by hard spheres, polymers and water.

This phenomenon is also described as an osmotic pressure drop in the overlapped region. As no polymer can be found on that zone, water molecules will diffuse to more polymer concentrated zones and particles will assemble.

Note that the polymer must be smaller than the colloidal particles in order to induce a depletion force. Nonetheless, if polymer's size is too small the resulting force will be insignificant.

Depletion forces are also found in non-spherical colloidal dispersions, such as disk-like or rod-like particles.²⁵ It is the case of LCLCs stacks, that can aggregate in N or M phases even though low concentration or high temperature conditions.²⁶

3.3.1. Polyethylene glycol (PEG) as a depleting agent

PEG, as a depleting agent, is used in all sort of colloidal systems from paints to viruses. Due to its hydrophilic and non-adsorbing character in water it is the depletant par excellence. It has been used in LCLCs systems with notable results.²⁷

Controlling polymers size is crucial as depletion force highly depends on it. PEG size in function of its molecular weight is described by the Flory-Huggins model (Equation 1).

$$R_g \approx \alpha M^{\nu} \quad (\text{Equation 1})$$

Where M is the molecular weight of the polymer, α a proportional constant and ν is the Flory exponent. This exponent is equal to 0.6 when the polymer is found in a good solvent, 0.5 at the Flory Temperature (θ) and less than 0.5 when it is found in a bad solvent.

4. OBJECTIVES

As explained in the introduction, control of colloidal systems is of great interest, and the phases they form under different conditions is a key point to understand and model their properties. Thus, the main goal of this project is to develop a new experimental tool to control colloidal systems such as LCLCs using thermoresponsive polymers as tuneable depleting agents.

The fulfilment of this objective is based on the following minor goals:

- To synthesize and characterize PNIPAM based materials in order to characterize their thermoresponsive behaviour.
- To correlate the depleting behaviour of PEG and PNIPAM in a salty solution by means of their radius of gyration.
- To study DSCG-Water phases and transitions in a confined system by a POM in the presence or absence of depleting agents.

5. EXPERIMENTAL SECTION

All the reagents were used as supplied without any further purification, reagent list is recorded in Appendix 1. The synthesized materials and water-based solutions prepared were stored in the fridge at 4°C and wrapped with Parafilm® “M” (Bemis Company, Inc.) to avoid degradation and evaporation.

5.1. PREPARATION OF PNIPAM BASED MATERIALS

5.1.1. Synthesis of microgel particles²⁵

The synthesis was performed under atmospheric pressure and with argon atmosphere. 45 mL of deionized water, 2.501 g of NIPAM (22.1 mmol), 24.9 mg of BIS (0.16 mmol) and 82.7 mg of acrylic acid (1.15 mmol) were mixed and stirred in a three-neck round bottom flask and heated up to 78 °C for 30 min. After that, 25.1 mg APS (0.11 mmol) in 5 mL deionized water solution was added and the mixture was stirred for another 30 min and then cooled down to room temperature. The solution was centrifugated (10 min, 7800 rpm, 25 °C) and supernatant was decanted, followed by re-suspending the hydrogel in deionized water. Overall, it was repeated five times.

5.1.2. Glass functionalization

The polymerization reaction was conducted on the glass surface. 0.6g of NIPAM (5.3 mmol) were solved in 30 mL deionized water and purged under argon flow for 30 min. Concurrently, two clean slides were rinsed with ethanol and submerged in a glass cuvette with 30 mL ethanol, 0.3 mL acetic acid and 0.15mL of 3-trimethoxysilylpropyl methacrylate (0.63 mmol) properly homogenized for 10 min. After that, the ethanol solution was removed. Then 10.5 µL of TEMED (0.07 mmol) and 28.5 mg of APS (0.12 mmol) were added to the monomer solution and then to the cuvette with the silanized glass. It is kept wrapped with Parafilm® “M” until further use.

5.2. LCLCs SOLUTIONS

Several DSCG-water solutions (Table 1) were prepared to study phases and transitions in function of temperature depleting agents. They were prepared by weight in a 2 mL Eppendorf.

Mixture	DSCG		Water [%]	PEG 4 kDa [mmol/kg]	PNIPAM 7 kDa [mmol/kg]
	[%]	[mol/kg]			
1	16.6	0.39	83.4	–	–
2	8.3	0.18	91.7	–	–
3	10.0	0.22	90.0	–	–
4	14.5	0.33	85.5	–	–
5	16.9	0.40	83.1	–	–
6	14.0	0.32	82.4	10.9	–
7	11.8	0.32	72.2	55.4	–
8	13.3	0.32	81.9	–	8.4
9	8.3	0.18	91.5	0.6	–
10	6.8	0.18	75.5	58.6	–
11	9.7	0.22	87.7	7.5	–
12	9.3	0.22	85.6	14.9	–
13	9.5	0.22	85.9	–	7.5
14	9.1	0.22	82.3	–	14.9

Table 1. DSCG water-based solutions prepared and their composition.

Firstly, different DSCG-Water mixtures (1-5) were prepared to study the phases at a given temperature, how do they transition, and which configuration take the condensate domains. Then, mixtures with PEG and PNIPAM (6-10) were prepared to study qualitatively the effect of depleting agents. Finally, a 10% LCLCs solution (3) was used to prepare equimolar PEG (11, 12) and PNIPAM (13, 14) mixtures.

Once weighted, the Eppendorf was wrapped and homogenized in a vortex at 3000 rpm for 2 min.

5.3. PREPARATION OF LC CELLS

Thin glass cells were prepared to study LCs phases under a POM. It allows to obtain images of better quality as there is less scattering. Nitrile gloves were used during the process, since scratches and skin grease damages glass coating and modifies LCs anchoring. Samples were always covered and blown with nitrogen after each step to avoid accumulation of dust particles.

5.3.1. Glass cleaning

Glass slides were cleaned thoroughly as the system studied is considerably sensitive. Substrates were cut into pieces with a diamond pen. They were first degreased mechanically with a diluted soap solution and then they were sonicated in the same solution for 10 min. Subsequently, the substrate was rinsed with deionized water. The liquid was removed and 40 mL of a piranha solution ($\text{H}_2\text{SO}_4:\text{H}_2\text{O}_2$ 3:1) were added for 20 min. Finally, the substrates were stored in deionized water before its further use.

5.3.2. PVA coating

PVA is a planar anchoring agent that homogenizes the glass surface and covers any nucleation sides like cracks and defects. Therefore, phase nucleation will be conducted on the bulk instead of the interfaces of the cell.

1% PVA in water solution was prepared and filtered (Nylon filter 0.22 μm) before its use. A clean glass was dried under a nitrogen flow and heated up to 130 °C for 10 min to remove any trace of water. The substrate was cleaned again with nitrogen to remove dust. The PVA solution was spin-coated onto the glass at 3000 rpm for 30 s. After that, the slide was heated up at 60 °C for 10 min and at 150 °C for 1 h to remove any trace of solvent. The plates were cooled down at room temperature and stored in a vacuum desiccator.

When used, the PVA coated glass was rubbed with a velvet cloth in a specific direction 20 times so that create a planar homogeneous disposition and a specific azimuthal orientation (always rubbed in the same direction, not back and forth).

5.3.3. Cell assembly

DSCG phases were observed in a glass cell that consisted on a solution sandwiched between two PVA-coated slides. Scheme of the cell assembly in Figure 10.

An 80 μm diameter Nylon wire (Maver Smart SLR Hi-Technology Monofilament Hook Line) was used to control glass slides spacing. Lateral gaps were filled with UV glue (Norland optical adhesive 81 from Norland Products, Inc.) to mechanically stabilize the cell. 15 μL of the selected solution were introduced by capillarity and the cell was sealed with UV glue once again to avoid water evaporation and ensure a known composition inside the sample.

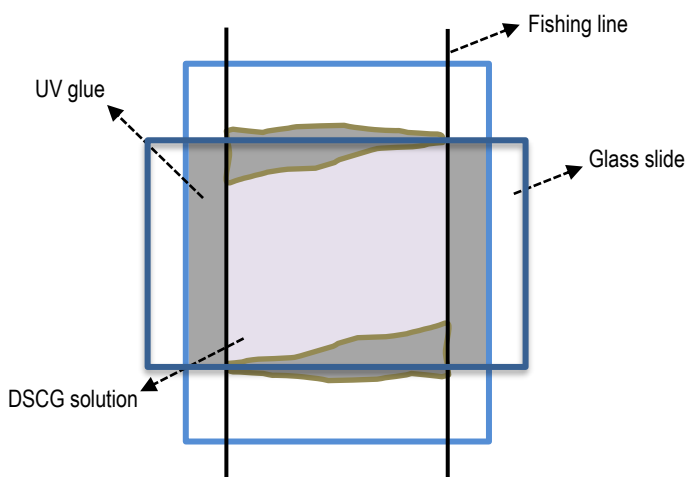


Figure 10. LC cell scheme.

Regarding to the sample injection, DSCG-Water and DSCG-Water-PEG mixtures were heated up to 45 $^{\circ}\text{C}$ and stirred in the vortex (3000 rpm, 10 s) before pipetting, to ensure a homogeneous composition (as in some cases two different phases were present at room temperature). With solutions containing PNIPAM, they were just homogenized in the vortex (3000 rpm 10 s) as heating would enhance PNIPAM-Water phase separation.

5.4. LC PHASES AND LC TRANSITION STUDY

The prepared cell was put in a temperature control device on the side of the POM, allowing an optimum temperature control while observing the sample. The POM incorporated camera (AVT

Marlin F131B IRF) captured black and white images of the system. Three different objectives were used: x4, x10 and x20.

The mK2000 INSTEC system (temperature control) is a Peltier cell, with an associated temperature error of 0.001 °C, although only the first decimal number was considered.

The sample was observed at room temperature and then heated up to complete I phase transition for 15 to 30 min, allowing a complete homogenization of the sample. In order to characterize the phase transition, two criteria were applied: (i) I phase was cooled down at 0.2 °C/min until the first condensed phases appeared, (ii) N or N+I phase was heated up at 0.2 °C/min until last N phase disappeared. Criteria (i) is used in Non-depletant and PEG containing solutions. Criteria (ii) is used for PNIPAM containing solutions, working below LCST. Sample were also studied at low temperatures (0-5 °C) and then heated up 40 °C at 0.2 °C once again.

5.5. INDIRECT SIZE MEASUREMENTS

As explained in the introduction, depletion force highly depends on the particles sizes of the studied system. For that reason, DSCG, PEG and PNIPAM solutions (Table 2) were analysed in a dynamic light scattering (DLS) instrument (Zetasizer Nano Series, Malvern Instruments, Inc.). Apart from commercial reagents, synthesized PNIPAM microgel particles were also characterized.

Number	Composition	Dispersant	Number	Composition	Dispersant
Ia	PEG 4 kDa 2%	M2B	Vb	PEG 20 kDa 2%	Deionized water
Ib	PEG 4 kDa 2%	Deionized water	VI	PEG 35 kDa 1%	M2B
II	PEG 6 kDa 2%	M2B	VII	DSCG 10%	Deionized water
III	PEG 10 kDa 2%	M2B	VIII	PNIPAM 7 kDa 1%	M2B
IV	PEG 12 kDa 2%	M2B	IX	PNIPAM microgel 1	Deionized water
Va	PEG 20 kDa 2%	M2B	X	PNIPAM microgel 2	Deionized water

Table 2. Solutions analysed with DLS.

Particles were solved in deionized water or M2B, which is a strong ionic buffer solution, to simulate a salty medium. 1.5 mL of the studied sample were injected through a 0.22 μm Nylon filter into a disposable plastic cuvette. Before measuring, the cell was stabilized for 2 min at the specified temperature.

To see in more detail this technique, see Appendix 2.

5.6. CONTACT ANGLE MEASUREMENTS

The thermoresponsive behaviour of a PNIPAM coating is related with its hydrophobic or hydrophilic character. Thus, water drops contact angle in its surface was measured at different temperatures. The temperature was controlled with a homemade Peltier cell and the working range 22 to 50 $^{\circ}\text{C}$.

The coated slide was dried under a nitrogen flow and heated up to 80 $^{\circ}\text{C}$ for 30 min to remove residual water. A 2 μL deionized water drop was put on the coated surface and the angle measured instantaneously, as the drop spread considerably in a few seconds.

6. RESULTS AND DISCUSSION

6.1. THERMORESPONSIVE MATERIALS

6.1.1. Microgel particles

A dense hydrogel was obtained from the free-radical polymerization of PNIPAM. When heated in a disposable cuvette, a white precipitate appeared at 30-31 $^{\circ}\text{C}$, slightly below the literature data.²⁵ A second synthesis was performed, obtaining a more transparent hydrogel but with the same LCST value.

DLS size measurements detected particles with a diameter of 300 up to 1000 nm for samples IX and X, which is considerably higher than the expected 150 nm.²⁵ Portions of these solutions were filtered through a 0.22 μm Nylon filter. But the resulting transparent solution did not provide any significant signal, so no microgel particles were smaller than 220 nm. Samples IX and X were

also studied at different temperatures (25, 28, 30, 32 and 35 °C), but no significant shift to lower diameters was observed.

PNIPAM-based copolymers are known to have softer thermoresponsive properties than pure PNIPAM polymers. Due to acrylic acid monomer, the molecule will shrink less considerably tuning its size in function of the monomer's ratio. The addition of a cross-linking agent (BIS) also affects the shape of the polymer in solution, as the structure will be more rigid, and it will not swell like a random coil.

Synthetic step was strictly followed twice according to Modlinska A. et al. procedure, obtaining the same results. The micrometric size values could be due to an aggregation of the particles while storing.

Under an optical microscope, dried microgel look like a uniform crosslinked structure, with non-discrete units. When adding water, it swelled and expanded, although it kept the linked structure. This observation suggests that the synthetic procedure lead to a macroscopic hydrogel instead of a microgel particles dispersions.

6.1.2. Functionalized glass

Glass surface was initially silanized with a methacrylate terminated silane derivate. Once linked, free-radical polymerization of NIPAM reacted with the acrylate group and linked the chain covalently to the glass surface.

Its properties were measured in a contact angle homemade apparatus, measuring water drops shape at different temperatures. Functionalized slides were completely dried before measuring, in order to remove residual water that could alter polymer response.

Theoretically, PNIPAM should be hydrophilic below LCST, whereas above that temperature it should be hydrophobic. Experimental data shows a slight increase in the contact angle values, although it does not show a clear LCST transition (Figure 11). It is considered a hydrophilic surface when contact angle is below 90°, so the functionalized glass is just decreasing its hydrophilic character instead of being hydrophobic.

Further work could be done measuring contact angles while cooling, to see whether it decreases or not. Thus, a reversible thermoresponsive character would be deduced.

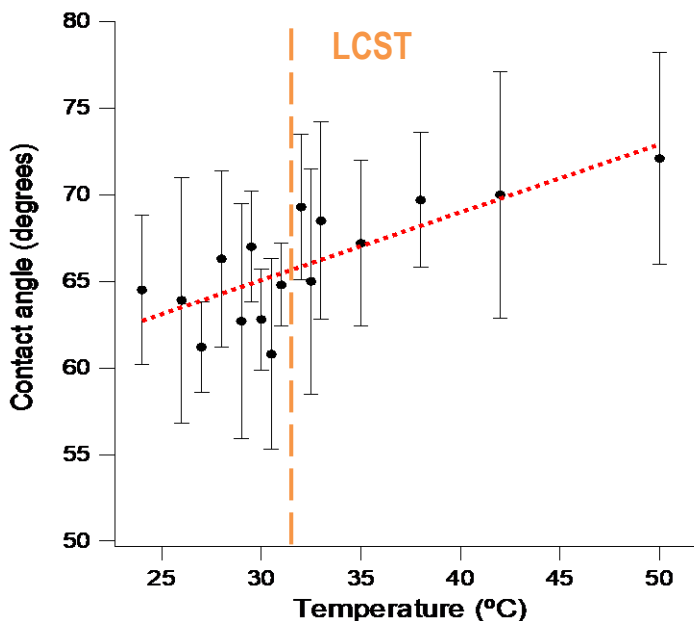


Figure 11. Water-Air-PNIPAM contact angle at different temperatures. LCST theoretical value in orange.

6.2. DLS MEASUREMENTS

6.2.1. PEG

PEG radius of gyration depending on the molecular weight is recorded in Figure 12. Its size increases when the molecular weight is increased, as expected. It scales in a factor of 0.47, low considering that PEG is supposed to be found in a good solvent. Flory-Huggins model predicts a $\nu=0.6$ for ideal polymers in good solvents, reference ν value for PEG in water is 0.58.²⁸

The Flory parameter indicates that PEG is found in a bad solvent in M2B. Due to its high ionic strength, water-PEG interactions might be affected. Because of that, its size has been also measured in deionized water. 4 kDa PEG in M2B (Ia) has a mean diameter of 3.4 nm, considerably lower than the 4.5 nm mean size in deionized (Ib). It confirms that PEG molecules size decreases in a salty solution.

Hydrophilic polymers shrink in high ionic strength media due to a competition for solvent molecules.²⁹ This explains the low experimental Flory parameter obtained and gives a better understanding of the PEG behaviour in salty solution like LCLCs.

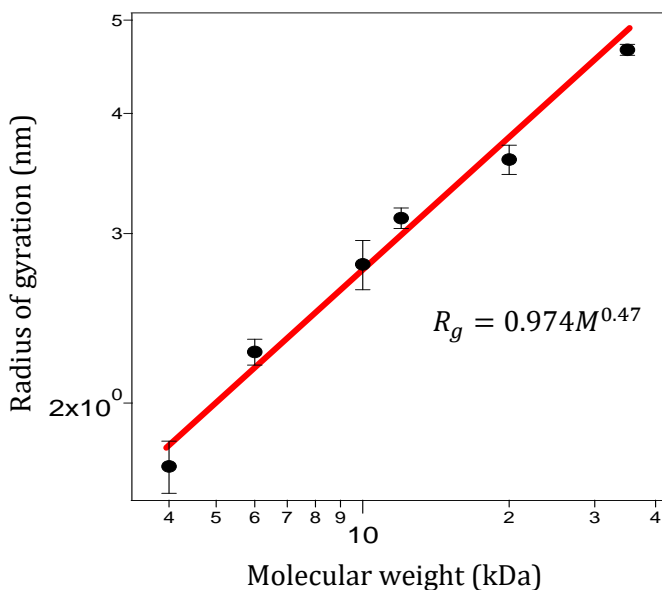


Figure 12. PEG size in M2B, samples I-VI.

6.2.2. PNIPAM

Commercial 7 kDa PNIPAM size has been measured in M2B (VIII) at different temperatures. The results show a slight increase in its size from 22 °C to 29 °C (Table 3). At 30 °C, they undergo LCST phase separation and shrink. Molecules start to aggregate immediately, so fold molecules size could not be measured. Aggregates size was not stable, histogram distribution varied considerably but always above 500 nm.

Temperature [°C]	22	24	25	26	28	29	30
Mean diameter [nm]	14.0	14.8	14.9	14.7	15.1	15.3	900

Table 3. Sample 8 mean size by temperature.

The LCST at 30 °C is slight below the common value, 32 °C. As commented in the previous chapter, ions in solution compete with the polymer for the solvent molecules. Thus, stabilising hydrogen bonds with water is harder in M2B than in pure water and the polymer shrink easier.

This kind of experiments are hard to reproduce, even with the same sample. When a temperature is set, different from room one, the system experiences a heat flow, even after equilibrating the sample temperature. In a solution, it involves convection flows, that will transport particles. As this technique is based on measuring the Brownian motion of the particles, convection flows can induce to errors and deviations. Thus, samples must be equilibrated enough time to ensure a minimum convection flow.

6.2.3. Size dependent depletion

DLS measurements has determined the in-situ size of PEG and PNIPAM in solution salty solutions. That value is related with the depletion force exerted to big colloidal particles in suspension. The bigger the diameter, the bigger the excluded volume will be, so large particles will be more attracted to each other.

PNIPAM mean size is larger than the heaviest measured PEG, so no correlation between sizes is obtained. Extrapolating the Flory-Higgins model found for PEG, a 77 kDa one would be equal to PNIPAM 7 kDa at 25°C. Despite this approximation, it is deduced that PNIPAM applies stronger depletion forces than PEG due to its bigger size below LCST. Above that temperature, PNIPAM molecules shrink, becomes hydrophobic and coagulates. Those polymeric aggregates do not cause depletion as they are not lyophilic, and its size exceed the length of the stacks.

That is why it is necessary for the polymers to be smaller than the colloidal particles. In Figure 13, DSCG size histogram is shown, exhibiting a huge polydisperse distribution from 1 to 100 nm. Values below 1 nm are below instrument tolerance, so they are virtually generated by the program and cannot be associated to the sample. DSCG 10% solution at 25 °C is isotropic and no condensed phases are present. I phase usually have broad size distributions, where stacks are small enough for not forming condensed domains. Once again, this technique does not provide fully reliable results, in this case due to its data treatment. The software assumes that measured particles are spherical., nothing further from the truth, are DSCG stacks are rod-like particles, with anisotropic Brownian motion due to its uniaxial symmetry.³⁰

Obviously, this histogram is modified at different temperatures and when adding depletants. Both polymers mean size are below 20 nm, the highest intensity peak in the DSCG histogram. Thus, it is qualitatively deduced that will deplete LCLCs stacks at 25 °C.

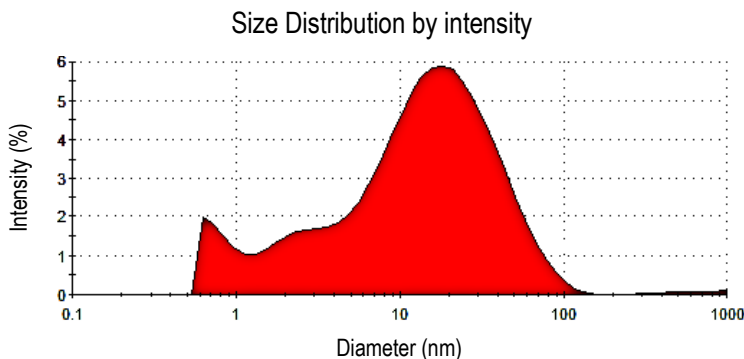


Figure 13. DSCG stacks size distribution, sample VII.

6.3. LCLCs PHASES AND TRANSITIONS

Comparing phase formation with and without depleting agents arises how important are those effects and how they can be tuned. Table 4 collects transition temperatures from N to I and M to I of the studied samples.

Mixture	Content	Transition temperature [°C]	Mixture	Content	Transition temperature [°C]
1	DSCG-Water	38.2 (N → I)	8	PNIPAM-DSCG-Water	31.3 (N → I)
2	DSCG-Water	6.2 (N → I)	9	PEG-DSCG-Water	8.0 (N → I)
3	DSCG-Water	16.5 (N → I)	10	PEG-DSCG-Water	33.2 (M → I)
4	DSCG-Water	31.1 (N → I)	11	PEG-DSCG-Water	21.3 (N → I)
5	DSCG-Water	38.7 (N → I)	12	PEG-DSCG-Water	31.7 (N → I)
6	PEG-DSCG-Water	42.1 (M → I)	13	PNIPAM-DSCG-Water	27.2 (N → I)
7	PEG-DSCG-Water	38.5 (M → I)	14	PNIPAM-DSCG-Water	30.5 (N → I)

Table 4. Transition temperatures of the studied samples.

6.3.1. DSCG-Water

Prepared solutions (1-5) consisted in I and I+N mesophases at room temperature. For solutions 1, 4 and 5, negative tactoids were observed at room temperature (Figure 14a and b), corresponding to a N+I where N is the continuous domain. Thus, their N to I transitions temperature were above room temperature. Regarding to solutions 2 and 3, they were completely dark at room temperature, meaning an I phase. After homogenization they transited at 6.2 °C and 16.5 °C respectively, forming positive tactoids (Figure 14c).

Prepared mixtures turned completely birefringent below 5 °C, so complete N transition was achieved. Heating the sample up to 45 °C for 15 to 30 min seem to homogenize properly, as subsequent transitions are instantaneous on the whole cell. Mixtures 1, 4 and 5 were heated up to 45 °C just before injecting, in order to take an isotropic liquid.

Positives tactoids birefringent images suggest a planar anchoring at the surface and a splay distortion of the director field. In some cases, twisting is also present (Figure 14c).

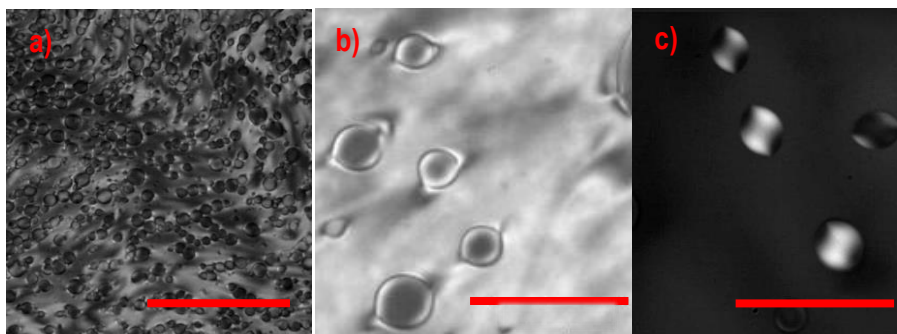


Figure 14. DSCG-Water mesophases: **a)** Negative tactoids, mixture 5 at 25 °C (scale bar 500 μm). **b)** Negative tactoids, mixture 5 at 25 °C (scale bar 100 μm). **c)** Positive tactoids, mixture 3 at 6 °C (scale bar 100 μm).

6.3.2. PEG-DSCG-Water

Mixtures 11 and 12 increased considerably their transition temperature with respect mixture 3, a non-containing PEG. Both mixtures show the same domains and shapes although they are found at different temperatures.

When cooled down below 5 °C, neither of both samples formed a continuous N phase. Instead of that, condensed phases folded small like Brussels sprouts (Figure 15a), some of them

coalesced. N cannot extend along the bulk because PEG is competing with him for the solvent. In bicomponent mixtures, all the containing water was able to mix with DSCG in the N phase. In this case, PEG retained water and banned N to extend. It had not been possible to distinguish whether the sprouts-like drops were nematic or hexagonal.

At 25 °C, mixture 12 consisted in bipolar nematic drops in coexistence with I (Figure 15b). From the axial point of view, they look like concentric circles with a cross at the centre. From the lateral point of view, they look like an opened watermelon.

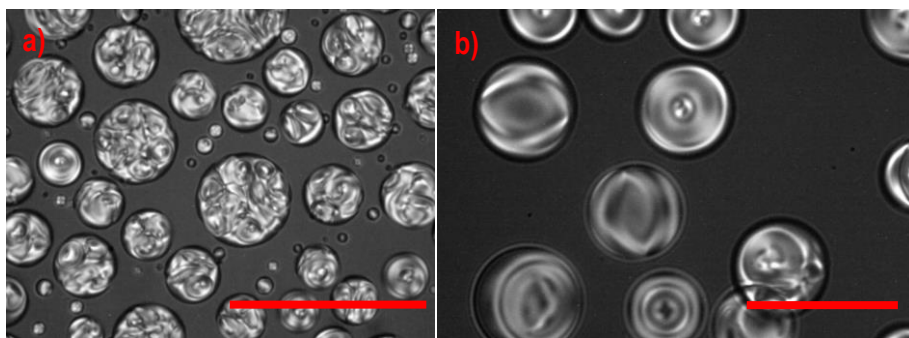


Figure 15. a) Mixture 12 at 5 °C (scale bar 500 μm). b) Bipolar droplets, mixture 12 at 25 °C (scale bar 50 μm).

M phases were detected in mixtures 6, 7 and 10. In mixture 6, M domains consisted on straight birefringent structures that bended to form toroids and then spherical drops (Figure 16a).

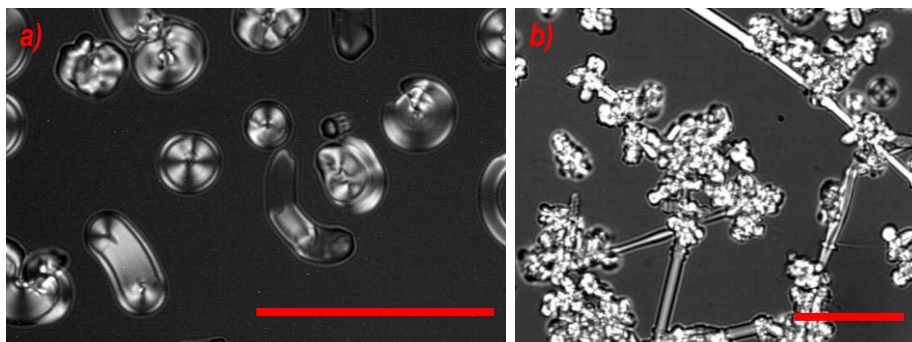


Figure 16. a) M-I coexistence, mixture 6 at 42 °C (scale bar 100 μm). b) DSCG star-like structure, mixture 10 at 33.2 °C (scale bar 100 μm).

Star-like structures were observed in mixtures 7 and 10 while cooling. Once a nucleus was formed, straight structures grew in different directions. Few radial drops appeared also, as shown in Figure 16b on the top-right corner. Like in less PEG concentrated solutions, no continuous condensed phases were formed at low temperatures, there were only M structures in an I background.

6.3.3. PNIPAM-DSCG-Water

Adding a thermoresponsive depleting agent to the colloidal systems allowed us to control the depletion force at a given temperature. As above LCST PNIPAM precipitates and the systems is heterogeneous, N to I transition is characterized by heating up the sample from N phases until no N domains.

According to DLS measurements, PNIPAM 7 kDa applies a stronger depletion force than PEG 4 kDa due to its bigger size. In mixture 13, nematic tactoids started to nucleate 6 °C above the equimolar prepared PEG solution (mixture 11). Sample 14, which is double concentrated PNIPAM with respect mixture 13, underwent N to I phase transition at 30.5 °C, just when PNIPAM aggregates formed (phase separation). However, its equimolar PEG solution (sample 12) transited 1 °C above mixture 14. This difference is associated with the lack of depletion forces on sample 14 above LCST. Depletion forces in PNIPAM samples only acted below 30 to 32 °C.

Mixtures 13 and 14 did not show defined nematic drops. Due to its strong depletion effect, most of the drops coalesced in sprouts-like domains (Figure 17a). Some bipolar nematic droplets had been observed before coalescence, in addition to tactoids (Figure 17b). At low temperatures,

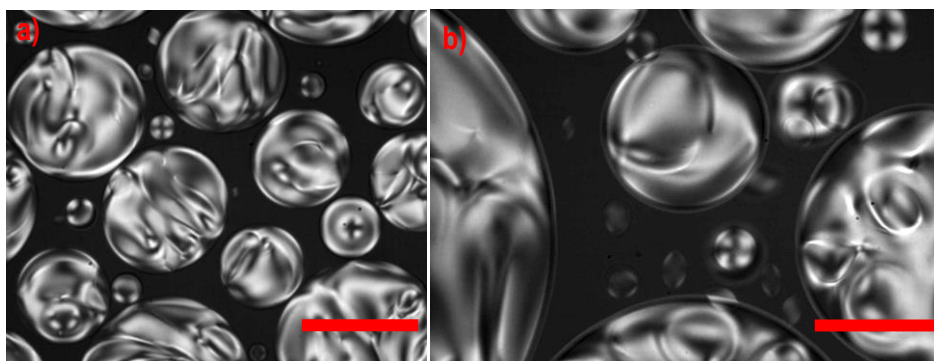


Figure 17. a) Mixture 14 at 25 °C (scale bar 100 μm). b) Mixture 13 at 20 °C (scale bar 50 μm).

no continuous N phase was formed, as in PEG mixtures. It is associated once again with the hydrophilic character of the PNIPAM and the competence for solvent molecules.

PNIPAM has demonstrated to be a thermoresponsive depleting agent whose phase transformation is reversible. However, some troubles have been detected while working on it. Firstly, when it undergoes the phase separation, polymer molecules aggregate and distort the image (Figure 18a). So, it is hard to study optically the system above that temperature. Secondly, the system seems to have memory, it does not homogenize the cell content when heated. Because of this, concentration gradients are created, and nematic phases tend to nucleate where the last one melted (Figure 18b). Finally, PNIPAM containing samples are hard to deal with. Below LCST the system is N+I, so it is not homogeneous. Above that temperature, there are no condensed phases but PNIPAM precipitates and aggregates. For that reason, mechanical homogenization was applied to these samples.

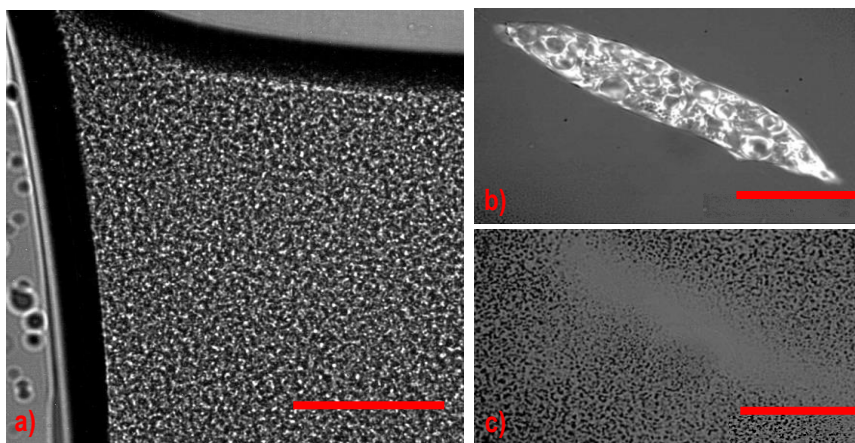


Figure 18. **a)** PNIPAM above LCST in a glass cell (scale bar 250 μm). **b)** A N domain in DSCG-Water-PNIPAM sample at 28 $^{\circ}\text{C}$ (scale bar 50 μm). **c)** The same region after heating for 5 min at 35 $^{\circ}\text{C}$. Black spots, PNIPAM aggregates, did not diffuse in the previous N domain zone (scale bar 50 μm).

7. CONCLUSIONS

According to the proposed goals, the experimental part of the project has consisted of three parts in order to determine the viability of controlling DSCG-Water systems by means of a thermoresponsive depletant.

Firstly, PNIPAM microgel particles and functionalized glass have been synthesized according to literature. No size change was detected in function of temperature in the microgel dispersion, even though LCST was identified at 30-31 °C. Particles aggregation during the synthetic procedure lead to a macroscopic hydrogel instead of discrete particles. Regarding to the PNIPAM functionalized glass, a slight increase of hydrophobicity was observed from 25 to 50 °C, but any abrupt transition did not happen from 30 to 33 °C.

Depleting agents' capacity has been related to its size. PNIPAM 7 kDa applied a depletion forces equivalent to a theoretical PEG 77 kDa, stronger than the studied PEG solutions. Thus, no correlation has been established between polymers' depleting power.

DSCG-Water I, N and M phases have been studied under the POM. Nematic droplets used to be bipolar drops, which meant a planar anchoring against the I phase and a splay deformation of the director field. N to I phase transition increased while increasing temperature or depleting agents' concentration. PNIPAM containing samples had higher transitions temperatures than PEG ones at the same molal concentration, confirming the stronger depletion effect. However, for those systems where N to I would be achieved above LCST, the loss of the depleting effect by the PNIPAM chains lead to a premature transition, whereas PEG-containing samples increased its transition temperature with no limitations.

Optical characterization of the system has led to the conclusion that PNIPAM is not a suitable depleting agent for DSCG-Water. Although its depletion force falls above LCST, which is of our interest, the aggregates formation and the memory of the cell suggest a non-reversible behaviour and implies added difficulties for characterizing the system. Thus, it would be better used in systems where the detected downsides are not so crucial.

8. REFERENCES AND NOTES

1. Semenov, A. N. & Shvets, A. A. Theory of colloid depletion stabilization by unattached and adsorbed polymers. *Soft Matter* **11**, 8863–8878 (2015).
2. Haw, M. D., Gillie, M. & Poon, W. C. K. Effects of phase behavior on the drying of colloidal suspensions. *Langmuir* **18**, 1626–1633 (2002).
3. Doublier, J., Garnier, C., Renarda, D. & Sanchezb, C. Protein-polysaccharide interactions. *Curr. Opin. Colloid Interface Sci.* **5**, 202–214 (2000).
4. Tortora, L. *et al.* Self-assembly, condensation, and order in aqueous lyotropic chromonic liquid crystals crowded with additives. *Soft Matter* **6**, 4157–4167 (2010).
5. Andrienko, D. Introduction to liquid crystals. *J. Mol. Liq.* **267**, 520–541 (2018).
6. Martin, J. D. *et al.* Metallotropic liquid crystals formed by surfactant templating of molten metal halides. *Nat. Mater.* **5**, 271–275 (2006).
7. Yamaguchi, A. Self-Assembly of Lyotropic Chromonic Liquid Crystal Mixtures. *Condensed Matter Physics Commons* (University of Colorado at Boulder, 2015).
8. Chami, F. & Wilson, M. R. Molecular order in a chromonic liquid crystal: A molecular simulation study of the anionic azo dye sunset yellow. *J. Am. Chem. Soc.* **132**, 7794–7802 (2010).
9. Vaughn, K. E., Sousa, M., Kang, D. & Rosenblatt, C. Continuous control of liquid crystal pretilt angle from homeotropic to planar. **194102**, (2007).
10. Yao, X. Studies on lyotropic chromonic liquid crystals in nematic and biphasic regions. (2011).
11. Verhoeff, A. A., Bakelaar, I. A., Otten, R. H. J., Van Der Schoot, P. & Lekkerkerker, H. N. W. Tactoids of plate-like particles: Size, shape, and director field. *Langmuir* **27**, 116–125 (2011).
12. Ny, T. & Corpora, F. M. C. United States Patent Office Patented Jaga. **4076**, 2–3 (1957).
13. Heskins, M. & Guillet, J. E. Solution Properties of Poly(N-isopropylacrylamide). *J. Macromol. Sci. Part A - Chem.* **2**, 1441–1455 (1968).
14. Clara-Rahola, J. *et al.* Structural properties of thermoresponsive poly(N-isopropylacrylamide)-poly(ethyleneglycol) microgels. *J. Chem. Phys.* **136**, (2012).
15. Teo, B. M., Prescott, S. W., Price, G. J., Grieser, F. & Ashokkumar, M. Synthesis of temperature responsive poly(N-isopropylacrylamide) using ultrasound irradiation. *J. Phys. Chem. B* **114**, 3178–3184 (2010).
16. Nagaoka, N. *et al.* Synthesis of Poly(N-isopropylacrylamide) Hydrogels by Radiation Polymerization and Cross-Linking. *Macromolecules* **26**, 7386–7388 (1993).
17. Ray, B. *et al.* Synthesis of Isotactic Poly(N -isopropylacrylamide) by RAFT Polymerization in the Presence of Lewis Acid . *Macromolecules* **36**, 543–545 (2003).
18. Jadhav, S. A., Brunella, V., Miletto, I., Berlier, G. & Scaronone, D. Synthesis of poly(N-isopropylacrylamide) by distillation precipitation polymerization and quantitative grafting on mesoporous silica. *J. Appl. Polym. Sci.* **133**, 1–8 (2016).
19. Zhang, Y., Furyk, S., Bergbreiter, D. E. & Cremer, P. S. Specific Ion Effects on the Water Solubility of Macromolecules : PNIPAM and the Hofmeister Series. *J. Am. Chem. Soc.* 14505–14510 (2005). doi:10.1021/ja0546424
20. Zaccarelli, E. On the molecular origin of the cooperative isopropylacrylamide) in water †. *Phys. Chem. Chem. Phys.* (2018). doi:10.1039/C8CP00537K
21. Park, B. R., Nabae, Y., Surapati, M., Hayakawa, T. & Kakimoto, M. Poly(N -isopropylacrylamide)-modified silica beads with hyperbranched polysiloxysilane for three-dimensional cell cultivation.

- Polym. J.* **45**, 210–215 (2012).
22. Guan, Y. & Zhang, Y. PNIPAM microgels for biomedical applications: From dispersed particles to 3D assemblies. *Soft Matter* **7**, 6375–6384 (2011).
 23. Lanzalaco, S. & Armelin, E. Poly(N-isopropylacrylamide) and Copolymers: A Review on Recent Progresses in Biomedical Applications. *Gels* **3**, 36 (2017).
 24. Tuinier, R., Fan, T. & Taniguchi, T. Current Opinion in Colloid & Interface Science Depletion and the dynamics in colloid – polymer mixtures. *Curr. Opin. Colloid Interface Sci.* **20**, 8–12 (2014).
 25. Modlinska, A., Alsayed, A. M. & Gibaud, T. Condensation and dissolution of nematic droplets in dispersions of colloidal rods with thermo-sensitive depletants. *Sci. Rep.* **5**, 1–10 (2015).
 26. Park, H. S., Kang, S. W., Tortora, L., Kumar, S. & Lavrentovich, O. D. Condensation of self-assembled lyotropic chromonic liquid crystal sunset yellow in aqueous solutions crowded with polyethylene glycol and doped with salt. *Langmuir* **27**, 4164–4175 (2011).
 27. Koizumi, R., Li, B.-X. & Lavrentovich, O. Effect of Crowding Agent Polyethylene Glycol on Lyotropic Chromonic Liquid Crystal Phases of Disodium Cromoglycate. *Crystals* **9**, 160 (2019).
 28. Zębacz, N., Wieczorek, S. A., Kalwarczyk, T., Fiałkowski, M. & Holyst, R. Crossover regime for the diffusion of nanoparticles in polyethylene glycol solutions: Influence of the depletion layer. *Soft Matter* **7**, 7181–7186 (2011).
 29. Baños, F. G. D. *et al.* Influence of ionic strength on the flexibility of alginate studied by size exclusion chromatography. *Carbohydr. Polym.* **102**, 223–230 (2014).
 30. Gonzalez, O. & Li, J. On the Hydrodynamic Diffusion of Rigid Particles of Arbitrary Shape with Application to DNA. *SIAM J. Appl. Math.* **70**, 2627–2651 (2010).
 31. Schurtenberger, P. & Urban, C. Characterization of Turbid Colloidal Suspensions Using Light Scattering Techniques Combined with Cross-Correlation Methods. *J. Colloid Interface Sci.* **207**, 150–158 (1998).
 32. Rodríguez Schmidt, R., Hernández Cifre, J. G. & García de la Torre, J. Translational diffusion coefficients of macromolecules. *Eur. Phys. J. E* **35**, (2012).

9. ACRONYMS

APS: Ammonium persulfate

BIS: N,N'-Methylenebis (acrylamide)

cmc: Critical micelle concentration

DLS: Dynamic Light Scattering

I: Isotropic

LC: Liquid crystal

LLC: Lyotropic liquid crystal

LCLC: Lyotropic chromonic liquid crystal

M: Hexagonal

M_w : Molecular weight

N: Nematic

NIPAM: N-isopropylacrylamide

PEG: Polyethylene glycol

PNIPAM: Poly(N-isopropylacrylamide)

POM: Polarized Optical Microscope

PVA: Polyvinyl alcohol

R_g : Radius of gyration

TEMED: N,N,N',N'-Tetramethylethylenediamine

UV: Ultraviolet

APPENDICES

APPENDIX 1: REAGENTS AND SUPPLIERS LIST

Reference	Name	Supplier	Composition	Additional information
J65122	Disodium cromoglycate	Alfa Aesar	98%	–
A16151	PEG 4,000	Alfa Aesar	–	–
81260	PEG 6,000	Ph ₂ -pybox	–	–
P6667	PEG 10,000	Sigma	–	–
81285	PEG 12,000	Sigma	–	–
95172	PEG 20,000	Sigma	–	–
81310	PEG 35,000	Sigma	–	–
724866	PNIPAM 7,000	Sigma	–	Carboxylic acid terminated
131085.1212	Ethanol	PanReac	96% v/v	(Reag. USP, Ph. Eur.) for analysis ACS
141077.1211	Hydrogen Peroxide	PanReac	33% w/v	Stabilized (USP, BP, Ph. Eur.) pure, pharma grade
–	Sulfuric acid	Lab grade	96%	–
22142500	Acetic acid	Acros Organics	98.8%	–
440159	Ethoxy silane	Sigma	98%	–
412781000	NIPAM	Acros Organics	99%	Stabilized
411019	N,N,N,N'-Tetramethylethylene diamine (TEMED)	Sigma	>99.5%	–
146072	N,N'-Methylenebis (acrylamide) (BIS)	Sigma	99%	–
1642250010	Acrylic acid	Acros Organics	98%	Stabilized
396760250	Polyvinyl alcohol (PVA)	Acros Organics	–	88% hydrolysed, Mw 20,000-30,000
A3678	Ammonium persulfate (APS)	Sigma	>98%	–

Table 5. Reagents used during the experimental procedure.

APPENDIX 2: DYNAMIC LIGHT SCATTERING (DLS)³¹

DLS is the most the most extended technique for determining the size of particles in the sub-micron region. It measures the particles' random motion (Brownian motion) and relates it to their size. Thus, active and driven particles cannot be measured by this method.

Solvent molecules bombards particles in suspension inducing a random motion. The smaller the particle, the faster the motion will be. On the other hand, the larger the particle, the slower it will be. Its random motion is related with the translational diffusion coefficient (D).³² Stokes-Einstein equation (Equation 2) establishes a model for this motion according to particles' hydrodynamic diameter (d_H) and D :

$$d_H = \frac{kT}{3\pi\eta D} \quad (\text{Equation 2})$$

Where k is the Boltzmann's constant, T the absolute temperature and η the viscosity of the medium.

Note that the size value is related to how the particles diffuses within the fluid, the hydrodynamic diameter. That value is the diameter of a spherical particle that will move with the same D , therefore non-spherical particles are assumed to be so. The assumption is reasonable for random coils, but nothing further from the truth for rod-like particles and stacks. Thus, the technique just provides a qualitative idea of that kind of samples.

How DLS work

The sample is put in front of the light source, normally a monochromatic laser. Light passes through the sample and is scattered partially due to the interaction with particles. A photomultiplier is placed at 173° with respect the exiting beam, it detects the scattered light, that results in a speckle pattern.

Each time, multiple particles are scattering, so out of phase waves will interact partially or fully destructive. As it also depends on the particles position, the speckle pattern is continuously varying. The measured intensity fluctuations are related with the size of the particles. The smaller the particle, the noisier the signal will be and more rapidly it will fluctuate.

This fluctuation is analysed with a correlator, that basically studies the correlation of the signal. The intensity of the signal at time t is compared to the intensity at subsequent times. Two signals will be strongly correlated if they are measured at small time differences. On the other hand, signals measured at two considerably different times will be less related.

The correlation of the signal is collected in the correlation function, that decays with time. Big particles tend to move slow and, as said before, light scattered fluctuates slow. Thus, the correlation function will decay at considerable high time values (Figure 19). On the other hand, small particles scattered light intensity fluctuates so rapidly that correlation function decays in a few μs (Figure 20).

There are two methods to obtain a size histogram from the correlation function. Cumulants analysis consists of fitting a single exponential to the correlation function, obtaining a mean size value and an estimate width of the distribution (polydispersity index). The other method consists of fitting a multiple exponential to obtain a size distribution of particle sizes (such us Non-Negative Least Squares (NNLS) or CONTIN).

Finally, a size distribution by intensity is obtained. It can be converted to volume or number distribution depending if we want to compare volume fractions or molar fractions.

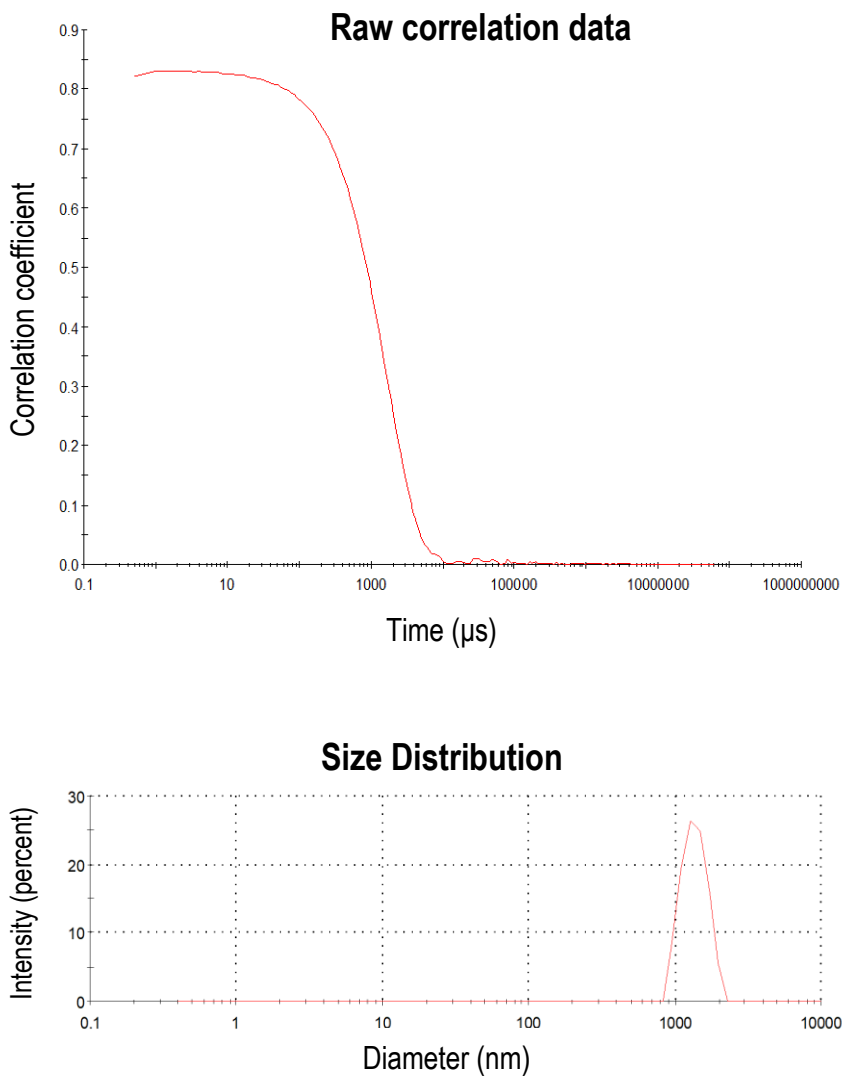


Figure 19. DLS analysis of big particles.

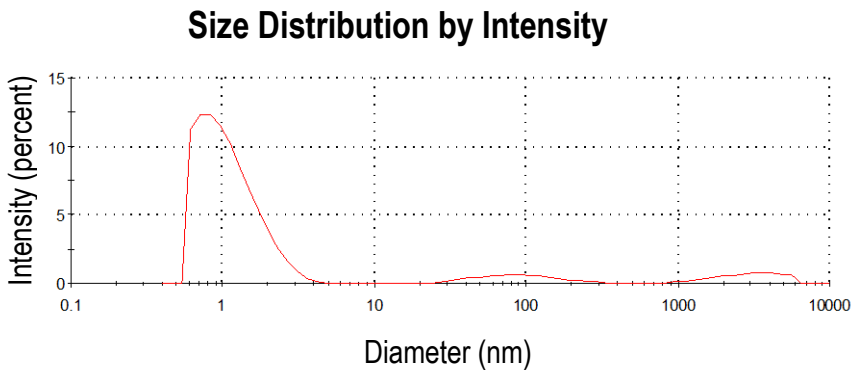
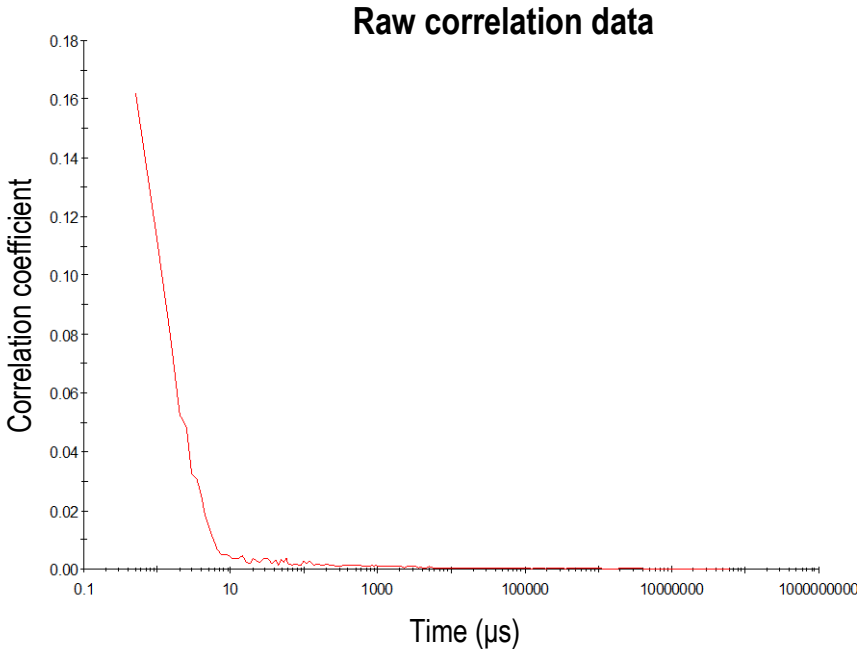


Figure 20. DLS analysis of small particles.

